





A Radio Pinwheel Emanating from WR 147

Luis F. Rodríguez^{1,2}, Jane Arthur¹, Gabriela Montes³, Carlos Carrasco-González¹ , and Jesús A. Toalá¹ 

¹ Instituto de Radioastronomía y Astrofísica, Universidad Nacional Autónoma de México, Apdo. Postal 3-72 (Xangari), 58089 Morelia, Michoacán, México; Lrodriguez@ira.unam.mx

² Mesoamerican Center for Theoretical Physics, Universidad Autónoma de Chiapas, Carretera Emiliano Zapata Km. 4, Real del Bosque (Terán), 29050 Tuxtla Gutiérrez, Chiapas, México

³ Unaffiliated

Received 2020 July 15; revised 2020 August 6; accepted 2020 August 8; published 2020 August 25

Abstract

Wolf–Rayet (WR) stars are evolved massive stars, presumably on their way to becoming supernovae. They are characterized by high luminosities and fast and dense stellar winds. We have detected signs of a radio continuum pinwheel associated with WR 147, a nitrogen-rich WR star with spectral subtype WN8. These structures are known to exist around a handful of late-type carbon-rich WR stars with massive companions where dust has formed in the zone where the two winds collide and produced a plume of dense gas and dust that is carried out with the WR wind. As the binary system rotates, an Archimedean spiral detectable in the infrared is formed. The resulting pinwheel contains information on wind speeds, wind-momentum ratio, and orbital parameters. However, WR 147 is a WN star and the formation of dust is unlikely, so a different emission mechanism must be at work. Our analysis of the data suggests that in this case the emission is dominantly of a nonthermal nature (synchrotron), although we cannot exclude the possibility that some clumps could be brighter in free–free emission. It is possible that the pinwheels associated with WN stars will be detectable only as nonthermal emitters at radio wavelengths. From the characteristics of the pinwheel we estimate a period of 1.7 yr for the binary system (the WN8 star and a companion yet undetected directly) that is responsible for the pinwheel.

Unified Astronomy Thesaurus concepts: [Binary stars \(154\)](#); [Wolf-Rayet stars \(1806\)](#); [Stellar winds \(1636\)](#)

1. Introduction

Wolf–Rayet (WR) stars, discovered in 1867 by Charles Wolf and Georges Rayet, are believed to represent the final stages in the evolution of very massive stars. These stars will end their lives as supernovae. There are two main types of WR stars: those with strong lines of nitrogen and helium (WN subtype) and those with strong carbon and helium lines (WC subtype). A third WO subtype with oxygen and carbon lines has been proposed (e.g., Crowther 2007; Trammer et al. 2015).

Over the years it has become clear that late-type carbon-rich WR stars with massive binary companions can produce spiral pinwheel structures detectable as infrared sources. The accepted model for these structures is that dust forms at the high-density interface between the colliding stellar winds. A plume of dust-rich material is then injected into the surrounding medium and, as the orbital motion wraps the plume, the pinwheel is formed. The first infrared pinwheel associated with a WR star was WR 104 (Tuthill et al. 1999). Over the years a few additional cases have been reported: WR 98a (Monnier et al. 1999), WR 112 (Marchenko et al. 2002), WR 140 (Monnier et al. 2002), Apep (Callingham et al. 2019), and possibly WR 118 (Millour et al. 2009). All these cases involve a WC star with an OB companion (in the case of Apep the binary is constituted by a WC star and a WN star; Callingham et al. 2020). This is not unexpected, as the WC winds are capable of nucleating graphite (a crystalline form of carbon and key component of interstellar dust) in the shock regions. By contrast, no WN star has been found to be associated with an infrared pinwheel structure.

It is known that relativistic electrons can be produced in the wind collision zone of massive binaries (e.g., White & Becker 1983; Pittard 2010; De Becker & Raucq 2013). Following the reasoning for the dust, one could expect to

detect synchrotron-emitting pinwheels in the case of WN stars. In this Letter we present high angular resolution, high-sensitivity radio observations of the WN star WR 147 that reveal a radio pinwheel of a nonthermal nature.

2. Observations

The observations were part of our Very Large Array (VLA) project 13B-258, made with the Karl G. Jansky VLA of the National Radio Astronomy Observatory (NRAO)⁴ in its highest angular resolution A-configuration during 2014 February 24. The flux and bandpass calibrator was J0137+331 and the phase calibrator was J2007+4029. The digital correlator of the VLA was configured in 48 spectral windows of 128 MHz width, covering the range of 12–18 GHz. Each spectral window is divided in 64 channels with individual spectral resolution of 2 MHz. The data were calibrated in the standard manner using the Common Astronomy Software Applications (CASA; McMullin et al. 2007) package of NRAO and the pipeline provided for VLA⁵ observations. In addition, the data were self-calibrated in phase and amplitude. Maps were made using a robust weighting (Briggs 1995) of -0.5 , searching to optimize the compromise between sensitivity and angular resolution.

3. Interpretation

In Figure 1 we show a color image of the WR 147 region made to emphasize the faint emission that traces the radio pinwheel. In Figure 2 we show the same data in the form of a

⁴ The National Radio Astronomy Observatory is a facility of the National Science Foundation operated under cooperative agreement by Associated Universities, Inc.

⁵ <https://science.nrao.edu/facilities/vla/data-processing/pipeline>

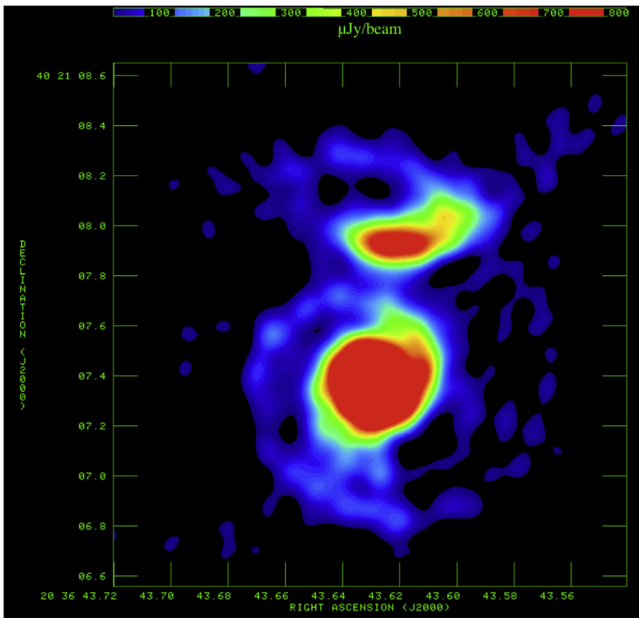


Figure 1. False-color image of WR 147 and its surroundings at 15 GHz. The color range is shown in the bar at the top of the figure and goes from 25 to $800 \mu\text{Jy beam}^{-1}$, with all flux densities above the latter value appearing saturated in red. This selection of color parameters emphasizes the faint spiral feature in the region. This same data is shown as a contour image in Figure 2.

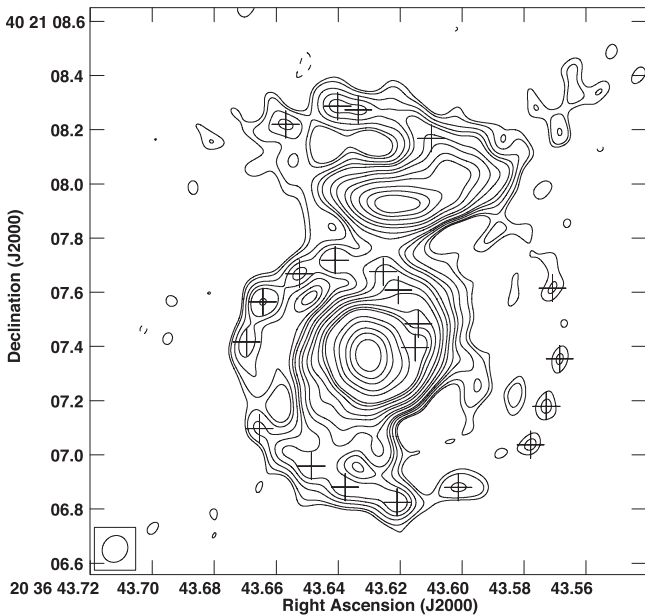


Figure 2. Contour image of WR 147 and its surroundings at 15 GHz. The beam ($0''.10 \times 0''.09$; $\text{PA} = -34^\circ$) is shown in the bottom-left corner. The contours are $-3, 3, 4, 6, 8, 10, 15, 20, 30, 40, 60, 80, 100, 200, 300, 500, 700,$ and $1000 \times 8 \mu\text{Jy beam}^{-1}$, the rms of the image. The crosses mark the positions of the local maxima used to describe the pinwheel.

contour image. Two well-known sources dominate the region: the first one, to the south, traces the thermal (free-free) emission of the wind from WR 147. The northern one, bow-shaped, traces the nonthermal (synchrotron) emission produced in the interaction zone of the winds of WR 147 with its B0.5V (Williams et al. 1997) companion. The spectral type of the northern companion is uncertain, with Niemela et al. (1998) favoring an O8-O9 V-III spectral type. We will refer to it as the OB star. This northern emission appears slightly to the south of

Table 1
Flux Densities and Spectral Indices of the Sources at 15 GHz

Source	Flux Density (mJy)	Spectral Index
WR 147	35.3 ± 0.1	$+0.55 \pm 0.04$
Bow Shock	3.6 ± 0.1	-1.0 ± 0.1
Pinwheel	3.5 ± 0.1	-1.1 ± 0.1^a

Note.

^a Determined from a combination of 15 and 22 GHz data.

the OB star because it traces the wind interaction zone and not the star itself (Abbott et al. 1986; Moran et al. 1989; Churchwell et al. 1992; Contreras et al. 1997; Williams et al. 1997; Skinner et al. 1999; Watson et al. 2002). It is known that these two sources are physically related because of the morphology of the bow shock and their common proper motions (Dzib & Rodríguez 2009).

The new component is the spiral structure that appears to emanate from WR 147. With respect to WR 147, the spiral starts at a position angle (PA) of $\sim -60^\circ$ and turns counter-clockwise. When it reaches a PA of $\sim 180^\circ$, the emission becomes faint and is detected only as a sequence of 4σ blobs. Interestingly, when the spiral reaches a PA of $\sim 340^\circ$, it seems to interact with the nonthermal bow shock located close to the northern OB companion and becomes relatively bright again. However, it is unclear if this enhancement is due to a physical interaction between both structures or to the superposition of their emissions. Finally, after a PA of $\sim 380^\circ$, the pinwheel is no longer detectable. PAs larger than 360° refer to points in the second crossing of the spiral with respect to the north.

Using the multi-frequency continuum imaging capability of CASA (Rau & Cornwell 2011) we can measure the spectral indices within the 12–18 GHz band of WR 147 and of the northern bow shock. These spectral indices are given in Table 1. The spectral index of the wind of WR 147, 0.55 ± 0.04 , is typical of an ionized thermal (free-free) wind (e.g., Panagia & Felli 1975). In contrast, the spectral index of the northern bow shock, -1.0 ± 0.1 , is characteristic of optically thin synchrotron. Determining the spectral index of the pinwheel is not as straightforward, given its faintness. We can measure the spectral indices directly with significant signal-to-noise ratio only in the segments spanning from -50° to 0° and 340° to 350° , obtaining values of -0.8 ± 0.2 and -1.0 ± 0.4 , respectively. To estimate the spectral index of the pinwheel as a whole we used our data at 22 GHz, also from project 13B-258, to make an image with the same angular resolution as the 15 GHz data presented here and determined the flux densities inside a polygon enclosing all the detectable pinwheel emission at 15 GHz. The pinwheel structure is marginal at 22 GHz, but a determination of its total flux density is possible. We obtain flux densities of 3.5 ± 0.1 mJy at 15 GHz and of 2.3 ± 0.1 mJy at 22 GHz. This implies a spectral index of -1.1 ± 0.1 , which is consistent with the value measured in the northern bow shock and in the brightest parts of the pinwheel.

The models for the nonthermal emission from a colliding-wind binary of Pittard et al. (2020) predict “cooling” of the relativistic electrons as they flow away from the shock. This cooling should be manifest in changes in the brightness and spectral index with distance from the shock, but our measurements are not accurate enough to compare with the

models. A rough calculation following Condon & Ransom (2016) and assuming energy equipartition and optically thin synchrotron emission gives a minimum magnetic field of ~ 5 mGauss for the segment spanning from -50° to 0° . A decay lifetime of order 10^3 yr is also derived for the relativistic electrons. This lifetime is much greater than the estimated orbital period (see Section 4). Under these assumptions the pinwheel can remain detectable over a relatively long distance from the star. However, this lifetime estimate assumes only losses by synchrotron radiation and is an upper limit, as other mechanisms (i.e., inverse Compton scattering of the stellar photons or expansion of the emitting region) could also make the radio emission decrease.

To characterize the pinwheel structure we determined the local maxima along the spiral, indicated by crosses in Figure 2. In Figure 3 we present an (x, y) plot with the positions of these maxima. The spiral appears to be of the Archimedean kind (radius proportional to angle); in Figure 3 we also show a radius versus PA plot derived from the positions using the equations

$$r = (x^2 + y^2)^{1/2}; \quad \text{PA} = -\tan^{-1}(x/y).$$

As can be seen, the radius versus PA plot can be approximately described by a straight line, supporting the Archimedean interpretation. A least-squares fit to these data gives

$$\left[\frac{r}{''} \right] = 0.30 \pm 0.01 + 0.53 \pm 0.01 \left[\frac{\text{PA}}{360^\circ} \right].$$

4. Determination of the Period of the Binary Producing the Pinwheel

WR 147 is located at a photometric distance of 650 pc (Morris et al. 2000). It is interesting to note that the Gaia parallax of WR 147 is negative (Gaia Collaboration et al. 2018), presumably because of the multiple nature of this object. From the fit derived above, the angular separation between consecutive turns of the pinwheel is $0''.53 \pm 0''.01$, which corresponds to a physical scale of 340 ± 7 au. Assuming that the pinwheel expands at 950 km s^{-1} , the velocity of the wind of WR 147 (Morris et al. 2000), we obtain a period of ~ 1.7 yr.

This result, combined with information available in the literature, suggests that WR 147 is at least a triple system. We first have the WN8 star itself, the dominant source in the system. About $0''.64$ to its north we have the OB star with wind that, in interaction with that of the WN8 star, produces the well-known nonthermal bow shock. Assuming a total mass of $40 M_\odot$ for the pair and using Kepler's third law, we roughly estimate a period of order 1300 yr for this system. We then have the star responsible, with the WN8 star, of producing the pinwheel, forming a system with an estimated period of 1.7 yr. Assuming a total mass of $30 M_\odot$ for this pair and using again Kepler's third law, we estimate a separation of ~ 4 au ($0''.006$) for the binary that produces the pinwheel.

Using Chandra observations, Zhekov & Park (2010a) determined that WR 147 is also a double X-ray source, with the X-ray components corresponding to the main radio ones. Although single WN2–6 are X-ray emitters, latter WN7–9 types are difficult to detect (Skinner et al. 2010, 2012; Toalá et al. 2018), prompting Zhekov & Park (2010a) to propose the presence of a companion. Zhekov & Park (2010b) detected a periodicity of 15 days in the X-ray emission from the WN8 star

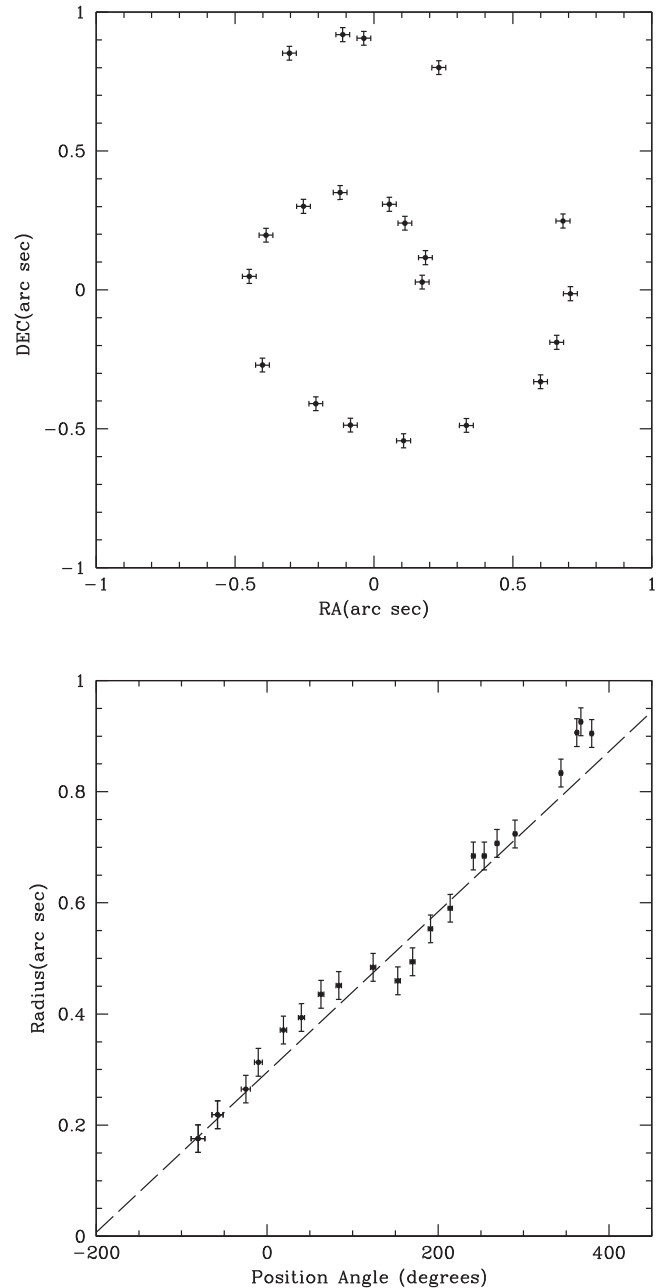


Figure 3. Top panel: positions of local maxima across the radio pinwheel with respect to the position of the peak emission of WR 147, R.A. (2000) = $20^{\text{h}}36^{\text{m}}43^{\text{s}}.630$; decl.(2000) = $40^{\circ}21'07''.37$. Bottom panel: radius of the pinwheel as a function of PA. The dashed line is the least-squares fit described in the text.

and proposed that this implies the presence of a very close star to WR 147 in the system. If confirmed, this would be a fourth star in the system. However, it is known that massive stars can present variability in their X-ray emission due to other phenomena (Oskinova 2016) and the reality of this fourth star is uncertain.

The finding that radio pinwheels can be detected in association with WN stars opens up the possibility of obtaining information on the orbital periods, wind speeds, and wind-momentum ratios in binaries containing this subclass of stars. As in the case of infrared pinwheels (Callingham et al. 2019), the detection of unusual patterns in the radio pinwheels may point to progenitors of long-duration gamma-ray bursts.

We thank an anonymous referee for a careful revision of our Letter that improved its clarity. L.F.R. acknowledges the financial support of PAPIIT-UNAM and of CONACyT (México). This research has made use of the SIMBAD database, operated at CDS, Strasbourg, France.

Facility: VLA.

Software: AIPS van Moorsel et al. (1996), CASA McMullin et al. (2007).

ORCID iDs

Carlos Carrasco-González  <https://orcid.org/0000-0003-2862-5363>

Jesús A. Toalá  <https://orcid.org/0000-0002-5406-0813>

References

- Abbott, D. C., Beiging, J. H., Churchwell, E., et al. 1986, *ApJ*, **303**, 239
- Briggs, D. S. 1995, *BAAS*, **27**, 1444
- Callingham, J. R., Crowther, P. A., Williams, P. M., et al. 2020, *MNRAS*, **495**, 3323
- Callingham, J. R., Tuthill, P. G., Pope, B. J. S., et al. 2019, *NatAs*, **3**, 82
- Churchwell, E., Bieging, J. H., van der Hucht, K. A., et al. 1992, *ApJ*, **393**, 329
- Condon, J. J., & Ransom, S. M. 2016, in *Essential Radio Astronomy*, ed. J. J. Condon & S. M. Ransom (Princeton, NJ: Princeton Univ. Press), 2016
- Contreras, M. E., Rodríguez, L. F., Tapia, M., et al. 1997, *ApJL*, **488**, L153
- Crowther, P. A. 2007, *ARA&A*, **45**, 177
- De Becker, M., & Raucq, F. 2013, *A&A*, **558**, A28
- Dzib, S., & Rodríguez, L. F. 2009, *RMxAA*, **45**, 3
- Gaia Collaboration, Brown, A. G. A., Vallenari, A., et al. 2018, *A&A*, **616**, A1
- Marchenko, S. V., Moffat, A. F. J., Vacca, W. D., et al. 2002, *ApJL*, **565**, L59
- McMullin, J. P., Waters, B., Schiebel, D., Young, W., & Golap, K. 2007, in *ASP Conf. Ser. 376, Astronomical Data Analysis Software and Systems XVI*, ed. R. A. Shaw, F. Hill, & D. J. Bell (San Francisco, CA: ASP), **127**
- Millour, F., Driebe, T., Chesneau, O., et al. 2009, *A&A*, **506**, L49
- Monnier, J. D., Tuthill, P. G., & Danchi, W. C. 1999, *ApJL*, **525**, L97
- Monnier, J. D., Tuthill, P. G., & Danchi, W. C. 2002, *ApJL*, **567**, L137
- Moran, J. P., Davis, R. J., Bode, M. F., et al. 1989, *Natur*, **340**, 449
- Morris, P. W., van der Hucht, K. A., Crowther, P. A., et al. 2000, *A&A*, **353**, 624
- Niemela, V. S., Shara, M. M., Wallace, D. J., Zurek, D. R., & Moffat, A. F. J. 1998, *AJ*, **115**, 2047
- Oskinova, L. M. 2016, *AdSpR*, **58**, 739
- Panagia, N., & Felli, M. 1975, *A&A*, **39**, 1
- Pittard, J. M. 2010, *MmSAI*, **81**, 341
- Pittard, J. M., Vila, G. S., & Romero, G. E. 2020, *MNRAS*, **495**, 2205
- Rau, U., & Cornwell, T. J. 2011, *A&A*, **532**, 71
- Skinner, S. L., Itoh, M., Nagase, F., et al. 1999, *ApJ*, **524**, 394
- Skinner, S. L., Zhekov, S. A., Güdel, M., et al. 2010, *AJ*, **139**, 825
- Skinner, S. L., Zhekov, S. A., Güdel, M., et al. 2012, *AJ*, **143**, 116
- Toalá, J. A., Oskinova, L. M., Hamann, W.-R., et al. 2018, *ApJL*, **869**, L11
- Tramper, F., Straal, S. M., Sanyal, D., et al. 2015, *A&A*, **581**, A110
- Tuthill, P. G., Monnier, J. D., & Danchi, W. C. 1999, *Natur*, **398**, 487
- van Moorsel, G., Kembell, A., & Greisen, E. 1996, in *ASP Conf Ser. 101, Astronomical Data Analysis Software and Systems V*, ed. G. H. Jacoby & J. Barnes (San Francisco, CA: ASP), 37
- Watson, S. K., Davis, R. J., Williams, P. M., et al. 2002, *MNRAS*, **334**, 631
- White, R. L., & Becker, R. H. 1983, *ApJL*, **272**, L19
- Williams, P. M., Dougherty, S. M., Davis, R. J., et al. 1997, *MNRAS*, **289**, 10
- Zhekov, S. A., & Park, S. 2010a, *ApJL*, **709**, L119
- Zhekov, S. A., & Park, S. 2010b, *ApJ*, **721**, 518